

: MR CISS 3 Volume Rendering ¹

: MR CISS 3 (volume rendering : VR)
 : 15 (10 , 5 ; 3 - 15 ; 6.5) 1.5 Tesla MR (Magnetom vision, Siemens, Erlangen, Germany) CISS (TR/TE/FA : 12.25ms/5.9ms/70 °) workstation (advanced workstation, volume analysis, Voxel 3.0.0, GE system)

VR . 3 VR

: 15 30 3 VR 25
 18 , 2 , 5 .
 1 1/2 1 1/3 . 15 ,
 6 , 4 , 3 , 2 ,
 가 2 . 13 , 6 ,
 5 , 4 , 3 . 12 , 7 ,
 가 5 , 4 , 2 . 14
 7 가 .

: 3 VR . MR CISS 3
 VR 2 가 .

가 8-20%
 (1) 가 2
 . 1940 Camp and Allen 2
 (2). 2
 3
 . 2 3
 , 3DFT CISS (three dimensional fourier transformation constructive interference in steady state) 2 가
 가 MR CISS 3
 (3- (volume rendering : VR) .
 5).

¹
²
³
 2003 6 11 2003 8 27 . 10 , 5 , 3 - 15 : 15 (6.5)

1.5 Tesla MR (Magnetom vision, Siemens, Erlangen, Germany) CISS

MR repetition time/ echo time/ flip angle 12.25 msec/5.90 msec/70°
 matrix 205 × 256, field of view 512 × 211, slab thickness 32.4 mm, 7 42 . MR CISS workstation (advanced workstation, volume analysis, Voxel 3.0.0, GE system) VR

(segmentation) (opacity curve) 가 가 175 가 400 (maximum opacity) 70% 3 VR 6 (anterior, posterior, superior, inferior, anterior oblique, posterior oblique) (Fig. 1).

30 VR , , , Jackler (1)

3 6 25 3 18 , 2 , 5 가 11 1/2 - 2/3 2 , 5 (Fig. 2, 3). 1 1/3 1 1/2 (Fig. 4, 5). 15 , (common crus aplasia) 6 , 4 , 3 , (short and broad) 2 , (cystic chamber) 가 2 (Fig. 2, 4). 6 , 13 , 5 , 4 , 3 (Fig. 2 - 6). 12 , 7 , (dilated crus) 가 5 , 4 , 2 (Fig. 2, 4 - 6). 7 가 8 (Table 1).

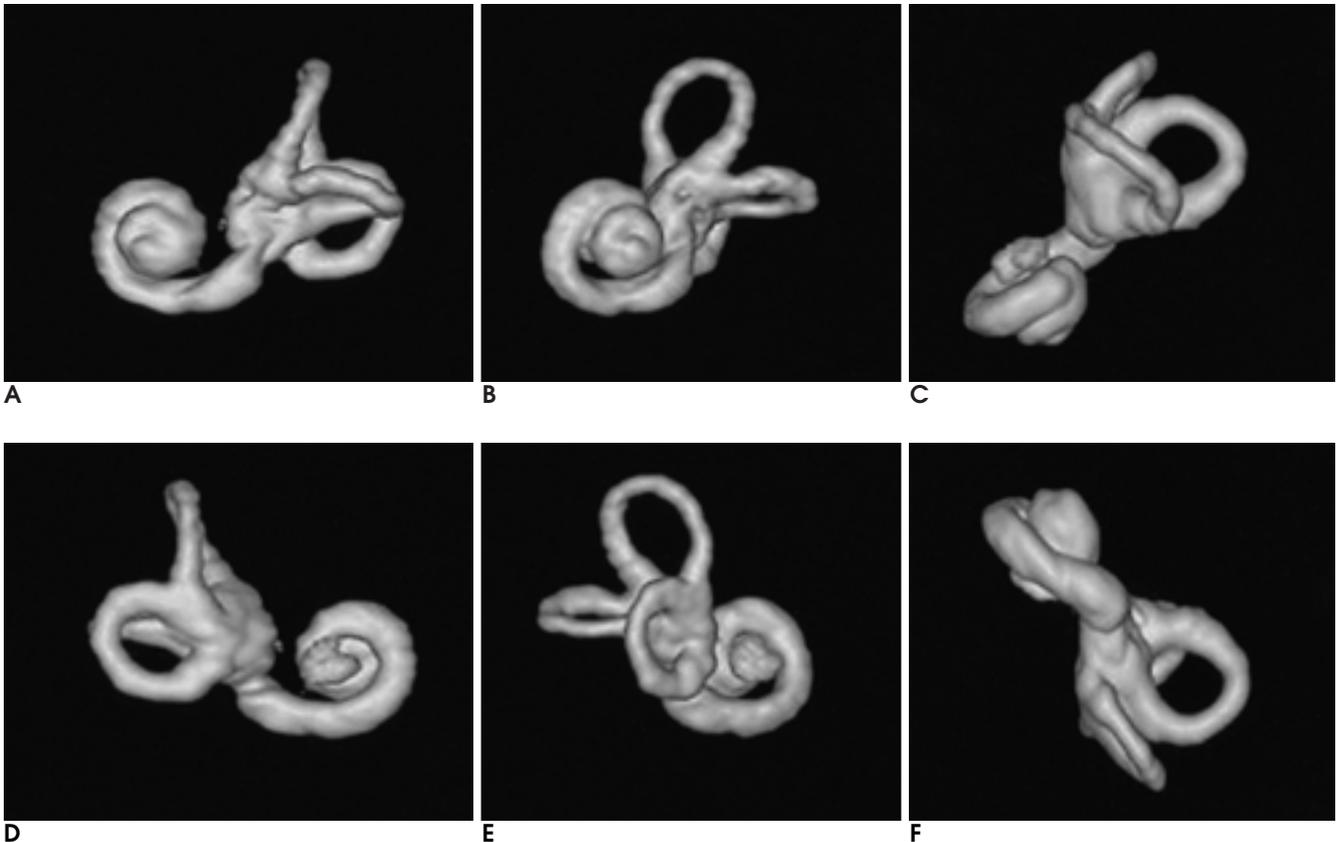


Fig. 1. Three dimensional volume rendering image using MR CISS axial image of normal left inner ear in a 10-year-old boy. **A)** anterior oblique view, **B)** anterior view, **C)** superior view, **D)** posterior oblique view, **E)** posterior view, **F)** inferior view.

3 가 가
 2 3/4 ,
 22 (6).

5
 , , 10 가
 가 26
 (1, 6). (1).
 Jackler (1)
 가
 (labyrinthin aplasia), (common cav -
 ity), (cochlea aplasia), (cochlea
 hypoplasia), (incomplete partition)

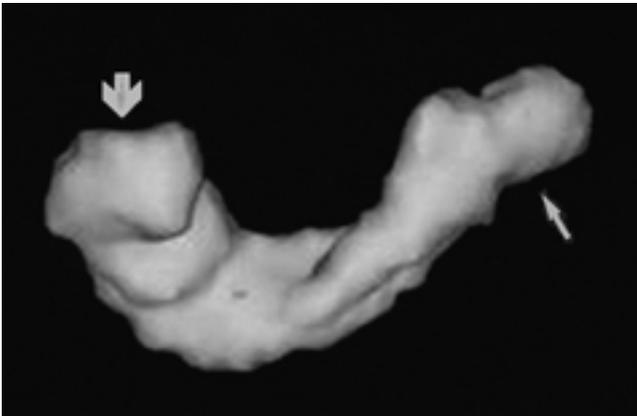


Fig. 2. A 4-year-old girl with hypoplasia of cochlea and aplasia of semicircular canal. Anterior oblique view of 3D volume rendering image shows a small bud like cochlea (large white arrow) and complete absence of semicircular canals (small white arrow).

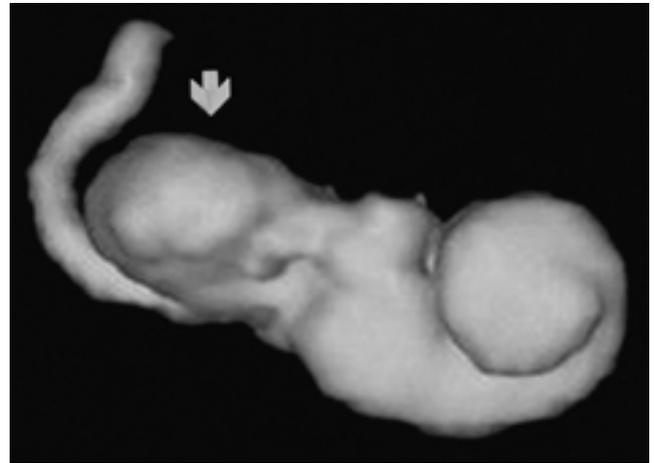


Fig. 4. A 2-year-old boy with multiple anomalies of cochlea and semicircular canals. Anterior oblique view of 3D volume rendering image shows incomplete partition of cochlea, common crus aplasia, hypoplasia of superior semicircular canal, broad shape of lateral semicircular canal (white arrow).



Fig. 3. A 10-year-old boy. Posterior oblique view of 3D volume rendering image shows severe hypoplasia of cochlea (large white arrow) and hypoplasia of posterior semicircular canal (small white arrow).

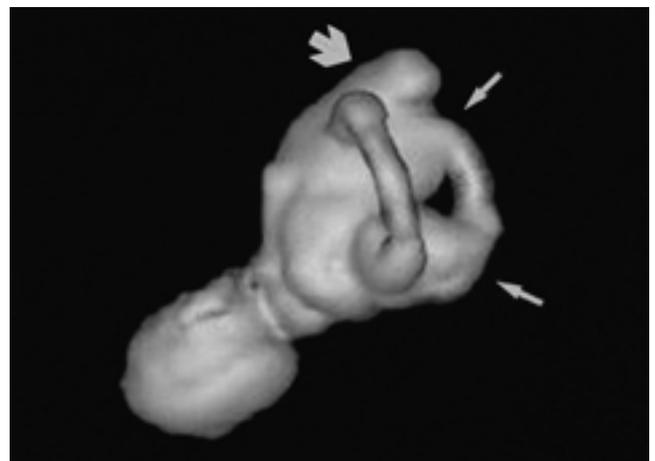


Fig. 5. A 2-year-old boy, Superior view of 3D volume rendering image shows incomplete partition of cochlea, short and broad shape of posterior semicircular (large white arrow) and dilated crus of lateral semicircular canal (small white arrow).

3 . 4
 5
 rudimentary bud 6
 가
 7
 1971 Mondini
 (enlarged vestibular aqueduct)
 2 가
 (7).
 가
 (1).
 18 가
 가 가

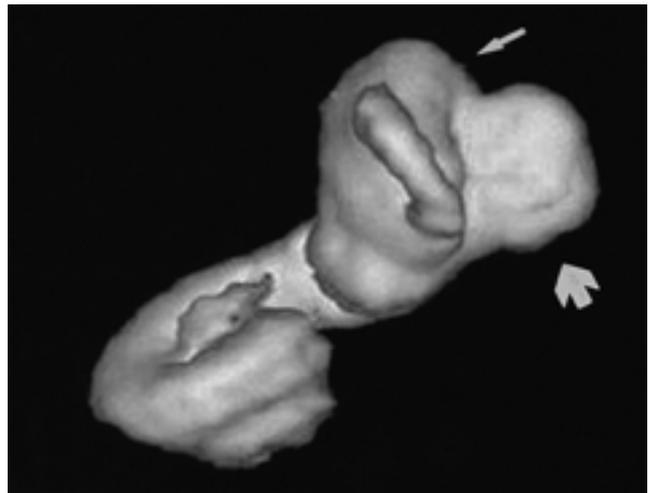


Fig. 6. A 5-year-old boy, Superior view of 3D volume rendering image shows short and broad shape of posterior (large white arrow) and lateral semicircular canal (small white arrow).

Table 1. Anomalies of Cochlea and Semicircular Canals on the Three Dimensional Volume Rendering Images in 15 Patients

No.	Sex	Age	R/L*	Cochlea [†]	SSCC [‡]	PSCC [‡]	LSCC [‡]
1	M	8	Rt	IP	aplasia	aplasia	B
			Lt	IP	CCA	CCA	S/B
2	M	10	Rt	SH	CCA	CCA	B
			Lt	SH	CCA	CCA	B
3	M	10	Rt	SH	N	H	N
			Lt	SH	N	H	N
4	M	2	Rt	IP	CCA, hypoplasia	CCA	B
			Lt	IP	N	S/B	dilated crus
5	F	11	Rt	IP	N	N	N
			Lt	IP	N	N	N
6	M	2	Rt	IP	N	N	N
			Lt	IP	N	N	N
7	M	3m	Rt	IP	N	N	S/B
			Lt	IP	N	N	N
8	M	5	Rt	IP	N	S/B	S/B
			Lt	IP	N	S/B	S/B
9	F	4	Rt	SH	aplasia	aplasia	aplasia
			Lt	H	aplasia	aplasia	aplasia
10	M	9	Rt	H	H,CCA	H,CCA	short/broad
			Lt	N	N	N	N
11	M	2	Rt	IP	N	N	N
			Lt	IP	N	aplasia	N
12	F	4	Rt	N	S/B	S/B	S/B
			Lt	N	S/B	S/B	S/B
13	M	12	Rt	N	cystic chamber	N	N
			Lt	N	cystic chamber	N	N
14	F	15	Rt	IP	N	N	dilated crus
			Lt	IP	N	N	dilated crus
15	F	10	Rt	IP	H	N	dilated crus
			Lt	IP	CCA	CCA	dilated crus

Note. - PSCC = posterior semicircular canal, LSCC = lateral semicircular canal, SSCC = superior semicircular canal

* : R/L, right or left; Rt, right; Lt, left

†: IP, incomplete partition; H, hypoplasia; SH, severe hypoplasia; N, normal

‡: CCA, common crus aplasia; B, broad; S/B, short and broad; H, hypoplasia; N, normal

12 11 가 . 3 (11, 12).
 , 가 CT MR 가 3
 10 6 가 . 3 shaded surface display (SSD),
 가 4 가 maximum intensity projection (MIP), volume rendering (VR)
 6 . 3 1 , 2 . 2
 2 . 5 . (13, 14).
 6 8 VR CT MR
 가 19-22 가 3 . VR
 가 가 (depth information)
 가 가 가 가 (13-16).
 가 3 SSD CT
 Parnes (8) Casselman (5), 가 . MR
 가 가 가
 가 가 가 가 가 (15). SSD
 가 VR 가 가
 가 가 가 (13, 18).
 가 가 가 MIP (density information)
 . CT 가 가 가 가
 , , , 가 가
 . 2
 (13, 17, 18).
 (9). MR VR SSD MIP 3
 CT
 가 (10). 가 가 가 . (apical widening)
 MR CISS (17, 18).
 0.5 mm MR CISS
 aqueduct) (vestibular aqueduct) (cochlea
 , , (10, 16).
 (3-5). MR CISS 3 VR
 가 3 가 (cochlea implanta-
 가 3 tion)

3 VR
가
(19, 20).
3 VR
MR CISS
3 VR 2
가

1. Jackler RK, Luxford WM, House WF. Congenital malformations of the inner ear: a classification made on embryogenesis. *Laryngoscope* 1987;97:2-14
2. Phelps PD. Ear dysplasia after Mondini. *J Laryngol Otol* 1994;108:461-465
3. Casselman JW, Kuhweide R, Deimling M, Ampe W, Dehaene I, Meeus L. Constructive interference in steady state-3DFT MR imaging of the inner ear and cerebellopontine angle. *AJNR Am J Neuroradiol* 1993;14:47-57
4. Casselman JW, Kuhweide R, Ampe W, Meeus L, Steyaert L. Pathology of the membranous labyrinth: comparison of T1- and T2- weighted and gadolinium-enhanced spin-echo and 3DFT-CISS imaging. *AJNR Am J Neuroradiol* 1993;14:59-69
5. Casselman JW, Kuhweide R, Ampe W, et al. Inner ear malformations in patients with sensorineural hearing loss: detection with gradient-echo (3DFT-CISS) MRI. *Neuroradiology* 1996;38:278-286
6. Mafee, MF. Congenital sensorineural hearing loss and enlarged endolymphatic sac and duct: role of magnetic resonance imaging and computed tomography. *Top Magn Reson Imaging* 2000;11:10-24
7. Lowe LH, Vezina LG. Sensorineural hearing loss in children. *Radiographics* 1997;17:1079-1093
8. Parnes LS, Chernoff WG. Bilateral semicircular canal aplasia with

near normal cochlear development. Two case reports. *Ann Otol Rhinol Laryngol* 1990;99(12):957-959

9. Brogan M, Chakeres DW, Schmalbrock P. High-resolution 3DFT MR imaging of the endolymphatic duct and soft tissues of the otic capsule. *AJNR Am J Neuroradiol* 1991;12:1-11
10. Westerhof JP, Rademaker J, Weber BP, Becker H. Congenital malformations of the inner ear and the vestibulocochlear nerve in children with sensorineural hearing loss: evaluation with CT and MRI. *J Comput Assist Tomogr* 2001;25:719-726
11. Schubert O, Sartor K, Forsting M, Reisser C. Three-dimensional computed display of otosurgical operation sites by spiral CT. *Neuroradiology* 1996;38:663-668
12. Seemann MD, Seemann O, Bonel H, et al. Evaluation of the middle and inner ear structures: comparison of hybrid rendering, virtual endoscopy and axial 2D source images. *Eur Radiol* 1999;9:1851-1858
13. Calhoun PS, Kuszyk BS, Heath DG, Carley JC, Fishman EK. Three-dimensional volume rendering of spiral CT Data: theory and method. *Radiographics* 1999;19:745-764
14. Udupa JK. Three-dimensional visualization and analysis methodologies: A current perspective. *Radiographics* 1999;19:783-806
15. Tomandl BF, Hastreiter P, Rezk-Salama C, et al. Local and remote visualization techniques for interactive direct volume rendering in neuroradiology. *Radiographics* 2001;21:1561-1572
16. Neri E, Caramella D, Cosottini M, et al. High-resolution magnetic resonance and volume rendering of the labyrinth. *Eur J Radiol* 2000;10:114-118
17. Krombach GA, Schmitz-Rode T, Tacke J, Glowinski A, Nolte-Ernsting CC, Gunther RW. MRI of the inner ear: comparison of axial T2-weighted, three-dimensional turbo spin-echo images, maximum-intensity projections, and volume rendering. *Invest Radio* 2000;35:337-342
18. Miyashita H, Isono M, Murata K, Nakayama K, Tanaka H, Ishikawa M. Three-dimensional magnetic resonance imaging findings of inner ear anomaly. *Acta Otolaryngol Suppl* 2000;542:67-70
19. Marsot-Dupuch K, Meyer B. Cochlea implant assessment: imaging issues. *Eur J Radiol* 2001;40:119-132
20. Murugasu E, Hans P, Jackson A, Ramsden RT. The application of three-dimensional magnetic resonance imaging rendering of the inner ear in assessment for cochlear implantation. *Am J Otol* 1999;20:752-757

Congenital Inner Ear Malformation: Three Dimensional Volume Rendering Image Using MR CISS Sequence¹

Jong Woon Song, M.D., In Sook Lee, M.D., Hak Jin Kim, M.D.,
Eui Kyung Goh, M.D., Lee Suk Kim, M.D.

¹Department of Diagnostic Radiology, College of Medicine, Pusan National University

²Department of Otolaryngorhinology, College of Medicine, Pusan National University

³Department of Otolaryngorhinology, College of Medicine, Dong-A University

Purpose: To evaluate three-dimensional volume-rendering of congenital inner-ear malformations using the MR CISS (Constructive Interference in Steady State) sequence.

Materials and Methods: MR CISS images of 30 inner ears of 15 patients (M:F=10:5; mean age, 6.5years) in whom inner-ear malformation was suspected were obtained using a superconducting Magnetom Vision System (Simens, Erlangen, Germany), with TR/TE/FA parameters of 12.25 ms/5.9 ms/70°. The images obtained were processed by means of the volume rendering technique at an advanced workstation (Voxtol 3.0.0; GE Systems, advanced workstation, volume analysis). The cochlea and three semicircular canals were morphologically evaluated.

Results: Volume-rendered images of 25 inner ears of 13 patients demonstrated cochlear anomalies in the form of incomplete partition ($n=18$), hypoplasia ($n=2$), and severe hypoplasia ($n=5$). For the superior semicircular canal, findings were normal in 15 ears, though common crus aplasia ($n=6$), hypoplasia ($n=4$), aplasia ($n=3$), and a short and broad shape ($n=2$) were also observed. The posterior semicircular canal of 13 ears was normal, but common crus aplasia ($n=6$), a short and broad shape ($n=5$), aplasia ($n=4$), hypoplasia ($n=3$) were also identified. Twelve lateral semicircular canals, were normal, but other images depicted a short and broad shape ($n=7$), a dilated crus ($n=5$), a broad shape ($n=4$), and aplasia ($n=2$). In 14 patients the anomalies were bilateral, and in seven, the same anomalies affected both ears.

Conclusion: Three-dimensional volume rendering images of the inner ear depicted various morphological abnormalities of the cochlea and semicircular canals. At that locations, anomalies were more complicated and varied than in the cochlea. Three-dimensional volume rendering imaging using the MR CISS technique provides anatomical information regarding the membranous labyrinth, and we consider this useful in the evaluation of congenital inner ear malformations.

Index words : MR CISS

Three-dimensional volume rendering

Congenital inner ear malformations

Address reprint requests to : Hak Jin Kim, M.D., Department of Diagnostic Radiology, Pusan National University Hospital

1-10, Ami-dong, Seo-ku, Busan 602-739, Korea.

Tel. 82-51-240-7371 Fax. 82-51-244-7534